



Vibration control of a flexible beam structure using squeeze-mode ER mount

W.J. Jung^a, W.B. Jeong^a, S.R. Hong^b, S.-B. Choi^{b,*}

^a *Vibration and Noise Laboratory, Department of Mechanical Engineering, Pusan National University, Pusan 609-735, South Korea*

^b *Smart Structures and Systems Laboratory, Department of Mechanical Engineering, Inha University, Incheon 402-751, South Korea*

Received 18 September 2001; accepted 17 April 2003

Abstract

This paper presents vibration control of a flexible beam structure supported by squeeze-mode electro-rheological (ER) mounts. After devising an appropriate size of the squeeze-mode ER mount, its field-dependent damping forces are evaluated at various exciting frequencies. The damping force controllability of the ER mount is also demonstrated by implementing a proportional integral derivative (PID) controller. The ER mounts are then incorporated with a flexible beam structure subjected to external excitations. The governing equation of the structural system is obtained and an optimal controller which consists of the position and velocity components of the beam structure as feedback signals is designed to attenuate the imposed vibrations. The controller is empirically realized and control responses such as beam acceleration are evaluated in time and frequency domains. In addition, the forces transmitted from the input point (exciting position) to the base plate (mount position) are investigated by applying control voltage and constant voltage.

© 2003 Elsevier Ltd. All rights reserved.

1. Introduction

Recently, with the aid of advanced technologies in computer and material sciences, high performance structural systems have been designed for application in various research fields such as space structures, bridges, and robotics. In particular, the emergence of the smart materials has accelerated successful development of the advanced structural system. So far, the smart materials include electro-rheological (ER) fluids, piezoelectric materials, shape memory alloys, and optical

*Corresponding author. Tel.: +82-32-860-7319; fax: +82-32-868-1716.

E-mail address: seungbok@inha.ac.kr (S.-B. Choi).

fibers. These smart materials are employed primarily to vibration control of distributed parameter systems operating under variable service conditions.

ER fluids undergo significant instantaneous reversible changes in material characteristics when subjected to electric potentials. The most significant change is associated with complex shear moduli of the material, and hence ER fluids can be usefully exploited in vibration-suppression situation where variable damping characteristics may be employed to effectively control the response by tailoring the properties of the ER fluid. The vibration control of flexible structures using the ER fluid can be achieved from two different methods. The first approach is to replace conventional viscoelastic materials by the ER fluid. So far, numerous researches have been undertaken in this way [1–3]. This method is very effective when the size of the flexible structure is small and the thickness of the structure is thin. The second approach to achieve vibration control of flexible structures is to utilize ER mount or ER damper. Originally, the idea of applying the ER mount to vibration control has been initiated in automotive engineering applications [4–7]. This idea can be easily exploited in structural vibration control [8–11]. This method is effective for the vibration control of the large size of the flexible structures. When the ER mount (or damper) is used for vibration control, operating mode of the mount can be classified by three different types: flow mode, shear mode, and squeeze mode [12]. In the flow mode, it is assumed that two electrodes are fixed, and hence vibration control is achieved by controlling the flow motion between two fixed electrodes [4]. In the shear mode, it is usually assumed that one of two electrodes is free to translate or rotate relative to the other, and hence vibration control is achieved by controlling shear force between two electrodes [9–11]. Unlike the former two modes, in the squeeze mode the electrode gap is varied and the ER fluid is squeezed by a normal force. Using this mode, various mounts or dampers can be devised for vibration control [13,14]. Squeeze film dampers using ER fluid were also shown to be effective for the reduction of vibration of rotor systems [15,16].

This paper presents vibration control of a flexible beam structure using squeeze mode ER mounts. An appropriate size of the squeeze mode ER mount is devised and its field-dependent damping force characteristics are experimentally evaluated. The ER mount is then applied to the flexible beam structure subjected to high frequency external excitation (up to 100 Hz). The governing equation of motion is formulated and an optimal controller to attenuate beam vibration as well as transmitted force from the input point (exciting position) to the base plate (mount position) is designed. The controller is experimentally realized and control responses such as beam acceleration are presented in both time and frequency domains. It is noted that none deals with the squeeze mode ER mount for vibration control of a flexible structure subjected to small amplitude and high-frequency excitations. It is remarked that the large engine supporting structural systems in the naval ships are normally subjected to small vibration magnitude at the elastic resonance modes, although the size of structural systems is large.

2. Squeeze-mode ER mount

The schematic configuration of the ER mount proposed in this work is shown in Fig. 1. The lower electrode is fixed to the base plate, while the upper electrode is to be moved up and down. Thus, the squeeze-mode motion of ER fluid occurs in the vertical direction. The coil spring is

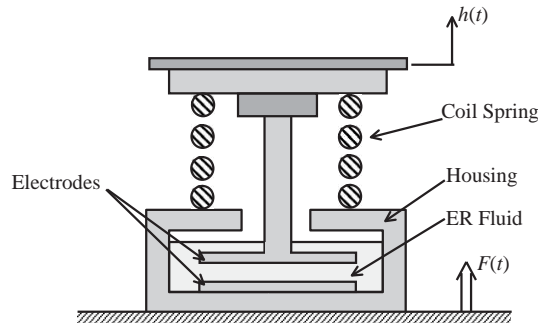


Fig. 1. Schematic configuration of the squeeze-mode ER mount.

attached to support a static mass which is the mass of a flexible beam structure. The total force of the proposed ER mount can be obtained by [17]

$$F(t) = kh(t) + c_f(t)\dot{h}(t) + f_{er}(t), \tag{1}$$

where

$$c_f(t) = \frac{3}{2} \frac{\pi\eta R^4}{(h_o + h(t))^3},$$

$$f_{er}(t) = \frac{4}{3} \frac{\pi R^3}{h_o + h(t)} \tau_y(E) \text{sgn}(\dot{h}(t)). \tag{2}$$

In the above, k is the stiffness constant of the coil spring, η is the viscosity of the ER fluid, $c_f(t)$ is the damping coefficient of the ER fluid in the absence of the electric field, $h(t)$ is the exciting displacement, h_o is the initial gap between lower and upper electrodes, and R is the radius of the circular electrode. $f_{er}(t)$ is controllable damping force owing to the electric field of E , and $\tau_y(E)$ is the field-dependent yield stress which is given by αE^β . Here, α and β are intrinsic values of the ER fluid to be experimentally determined. In this work, for the ER fluid chemical starch and silicone oil whose viscosity is 30 cSt are used for particles and base liquid, respectively. The intrinsic values of α and β are experimentally obtained by 427 and 1.2, respectively, at room temperature [18].

By considering the mass of the beam structure, an appropriate size of the ER mount is manufactured as shown in Fig. 2. The radius of circular electrode is designed to be 15 mm and the initial gap is fixed by 3 mm. The electrodes are made of duralumin, and the spring constant of the coil spring is 4 kN/m. The height and outer diameter of the ER mount are 150 and 100 mm, respectively. Fig. 3 presents time responses of the measured force of the ER mount. The excitation frequency is 75 Hz, and the excitation amplitude is $\pm 40 \mu\text{m}$. We clearly see the damping force is increased as the applied voltage increases. For instance, the force 0.6N at 1 kV is increased up to 2.7N by applying the voltage of 4 kV. We also tested the force at three different exciting frequencies and presented the results in Fig. 4. We observe that slightly higher force is obtained at the higher excitation frequency with the same input voltage. This can be easily expected from the ER mount model given by Eq. (1).

We see from Fig. 3 that the response time of the proposed squeeze-mode ER mount due to the step input voltage is fairly fast. Thus, the damping force controllability in a fast motion is

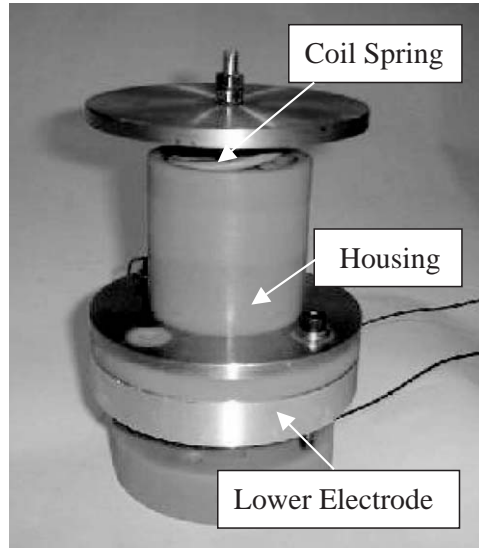


Fig. 2. Photograph of the squeeze-mode ER mount.

investigated in this work. The desired damping force is imposed in the microprocessor, and a simple PID controller is designed so that actual damping force tracks to the desired one by applying an appropriate control voltage. So, the control electric field is determined by

$$E(t) = k_P e(t) + k_I(t) \int e(t) dt + k_D \dot{e}(t), \quad (3)$$

where

$$e(t) = F(t)_{desired} - F(t)_{actual},$$

$$E(t) = V(t)/h(t). \quad (4)$$

In Eq. (3), k_P , k_I and k_D are proportional, integral and derivative control gains, respectively. Unlike the flow-mode or shear-mode ER mount, the electrode gap of the squeeze-mode ER mount varies with respect to the time. Therefore, the control electric field given by Eq. (3) should be converted to the actual voltage $V(t)$ by considering the time varying $h(t)$ in a real-time closed-loop manner. For the implementation, the control gains of k_P , k_I and k_D are chosen by 5.8, 0.002, and 0.01, respectively. Fig. 5 presents the damping force controllability of the ER mount. The desired damping force trajectory which is expressed by $2 \sin(2\pi \cdot 70 \cdot t)N$ is well tracked by the actual one. This result directly indicates that the damping force of the squeeze-mode ER mount can be effectively controlled by the electric field up to 70 Hz. This control frequency of 70 Hz is relatively high compared with the flow or shear mode ER mount [7]. The high control performance of the squeeze-mode ER mount is now applied to vibration control of a flexible beam structure.

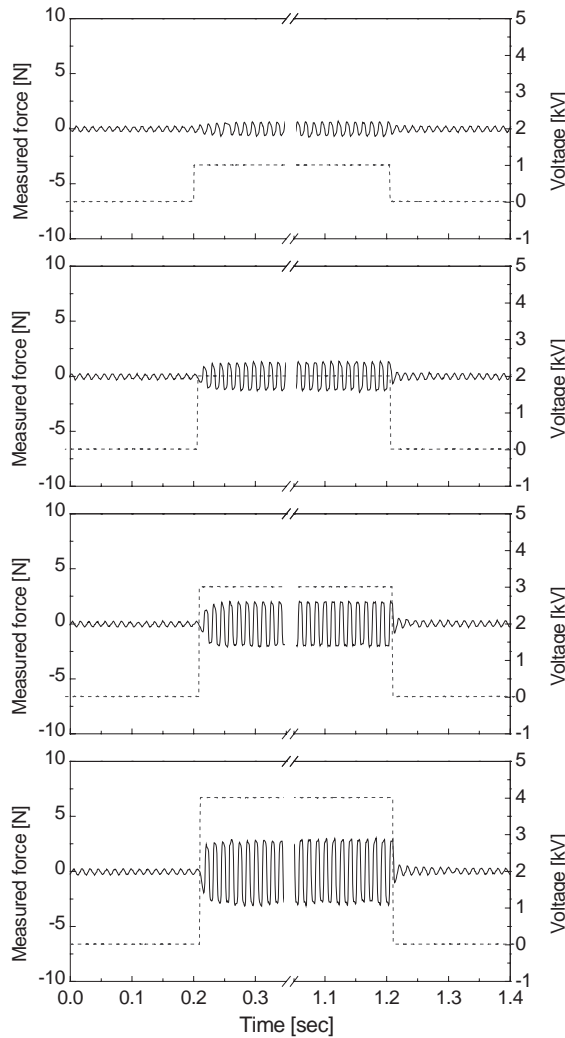


Fig. 3. Time responses of the field-dependent force of the ER mount. —: force; - - - -: voltage.

3. Modelling of beam structure

Consider a flexible beam structure which has a continuous and uniform beam of length L as shown in Fig. 6. A beam is supported by two spring mounts and two ER mounts. The spring mounts are positioned at l_1 and l_5 , while the ER mounts at l_2 and l_4 . When the Bernoulli–Euler beam theory is applied, the kinetic energy T , potential energy V and non-conservative work W_{NC} are obtained by

$$T = \frac{1}{2} \int_0^L \rho \left(\frac{\partial y(x, t)}{\partial t} \right)^2 dx + \frac{1}{2} (m_1 \dot{y}(l_1, t)^2 + m_2 \dot{y}(l_2, t)^2 + m_4 \dot{y}(l_4, t)^2 + m_5 \dot{y}(l_5, t)^2), \quad (5)$$

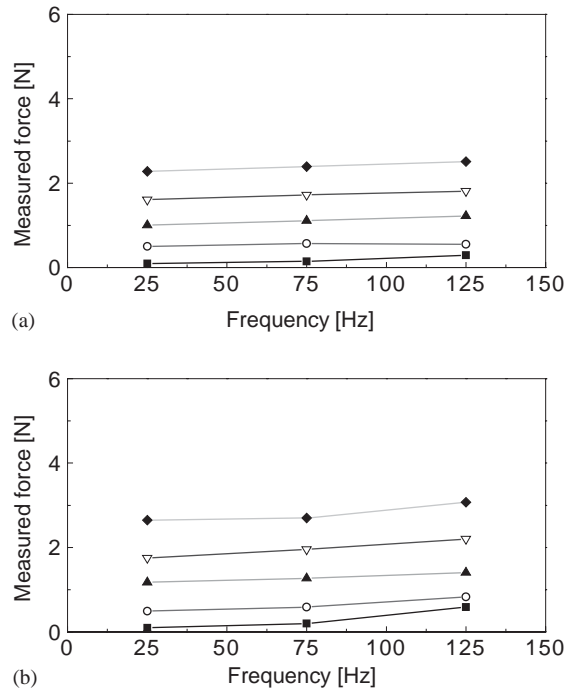


Fig. 4. Frequency response of the field-dependent force of the ER mount. (a) Excitation amplitude: $\pm 20 \mu\text{m}$ (b) excitation amplitude: $\pm 40 \mu\text{m}$. —■—: 0 kV, —○—: 1 kV, —▲—: 2 kV, —▽—: 3 kV, —◆—: 4 kV.

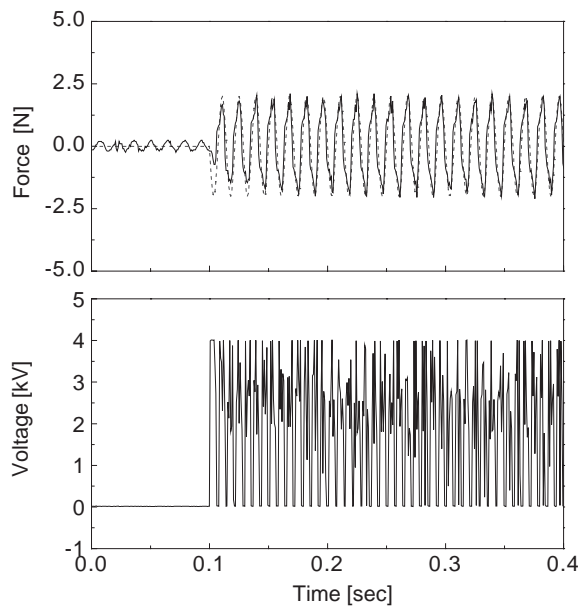


Fig. 5. Force control responses of the ER mount. - - - - -: desired, —: actual.

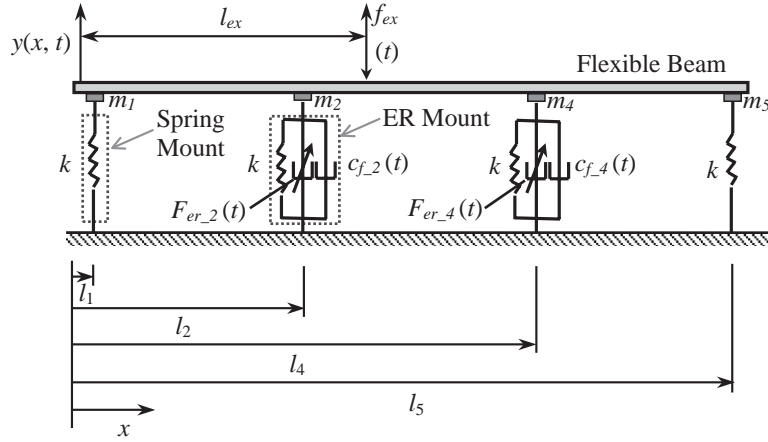


Fig. 6. Schematic configuration of the beam structure supported by the ER mount.

$$V = \frac{1}{2} \int_0^L EI \left(\frac{\partial^2 y(x, t)}{\partial x^2} \right)^2 dx + \frac{1}{2} k (y(l_1, t)^2 + y(l_2, t)^2 + y(l_4, t)^2 + y(l_5, t)^2), \quad (6)$$

$$W_{nc} = \int_0^L (F_{ex}(x, t) - F_{vis}(x, t) - F_{er}(x, t)) dx, \quad (7)$$

where

$$\begin{aligned} F_{ex}(x, t) &= \delta(x - l_{ex}) f_{ex}(t), \\ F_{vis}(x, t) &= \delta(x - l_2) f_{vis_2}(t) + \delta(x - l_4) f_{vis_4}(t), \\ F_{er}(x, t) &= \delta(x - l_2) f_{er_2}(t) + \delta(x - l_4) f_{er_4}(t), \\ f_{vis_j}(t) &= c_{f-j}(t) \dot{y}(l_j, t) = \frac{3}{2} \frac{\pi \eta R^4}{(h_o + y(l_j, t))^3} \dot{y}(l_j, t), \\ f_{er_j}(t) &= \frac{4}{3} \frac{\pi \eta R^3}{h_o + y(l_j, t)} \tau_y(E) \text{sgn}(\dot{y}(l_j, t)). \end{aligned} \quad (8)$$

In the above, ρ is the beam mass per unit length, EI is the effective bending stiffness, k is the spring constant, m_i is the mass of upper part of each mount, $f_{ex}(t)$ is the exciting force, $f_{vis_j}(t)$ is the damping force of the ER mount due to the viscosity of the ER fluid, and $f_{er_j}(t)$ is the damping force of the ER mount due to the yield stress of the ER fluid which is controllable damping force by the electric field. In Eq. (8), $\delta(\cdot)$ represents the Dirac delta function.

By employing energy equations and Hamilton's principle, the governing equations of motion for transverse deflection $y(x, t)$ and associated boundary condition are obtained as follows [18].

$$\begin{aligned} EI y^{(iv)} + \rho \ddot{y} &= 0, \quad 0 \leq x \leq l_2, l_4 \leq x \leq L, \\ EI y^{(iv)} + \rho \ddot{y} &= -F_{vis}(x, t) - F_{er}(x, t) + F_{ex}(x, t), \quad l_2 \leq x \leq l_4, \\ (EI y''' + ky + m_1 \ddot{y})|_{x=0} &= 0, \quad EI y''|_{x=0} = 0, \end{aligned} \quad (9)$$

$$\begin{aligned}
EIy''''|_{x=l_2^-} &= (EIy'''' + ky + m_2\ddot{y})|_{x=l_2^+}, & EIy''|_{x=l_2^-} &= EIy''|_{x=l_2^+}, \\
(EIy'''' - ky - m_4\ddot{y})|_{x=l_4^-} &= EIy''''|_{x=l_4^+}, & EIy''|_{x=l_4^-} &= EIy''|_{x=l_4^+}, \\
(EIy'''' - ky - m_5\ddot{y})|_{x=L} &= 0, & EIy''|_{x=L} &= 0, \\
y(l_2^-, t) &= y(l_2^+, t), & y'(l_2^-, t) &= y'(l_2^+, t), \\
y(l_4^-, t) &= y(l_4^+, t), & y'(l_4^-, t) &= y'(l_4^+, t).
\end{aligned} \tag{10}$$

By introducing the i th modal co-ordinate $q_i(t)$ and mode shape $\phi_i^{(i)}(x)$ at each section, the transverse deflection $y(x, t)$ is represented using the mode summation method as follows:

$$\begin{aligned}
y(x, t) &= \sum_{i=0}^{\infty} \Phi_i^{(1)} q_i(t), & 0 \leq x \leq l_2, \\
y(x, t) &= \sum_{i=0}^{\infty} \Phi_i^{(2)} q_i(t), & l_2 \leq x \leq l_4, \\
y(x, t) &= \sum_{i=0}^{\infty} \Phi_i^{(3)} q_i(t), & l_4 \leq x \leq L.
\end{aligned} \tag{11}$$

Substituting Eq. (11) into Eqs. (5)–(7) and then by using the Lagrange equation, a decoupled ordinary equation for each mode is derived by

$$\ddot{q}_i(t) + 2\zeta_i\omega_i\dot{q}_i(t) + \omega_i^2q_i(t) = \frac{Q_i(t)}{I_i} + \frac{Q_{exi}(t)}{I_i}, \tag{12}$$

where

$$\begin{aligned}
Q_i(t) &= -\phi_i(l_2)f_{vis-2}(t) - \phi_i(l_4)f_{vis-4}(t) - \phi_i(l_2)f_{er-2}(t) - \phi_i(l_4)f_{er-4}(t), \\
Q_{exi}(t) &= \phi_i(l_{ex})f_{ex}(t), \\
I_i &= \rho \left[\int_0^{l_2} (\Phi_i^{(1)}(x))^2 dx + \int_{l_2}^{l_4} (\Phi_i^{(2)}(x))^2 dx + \int_{l_4}^L (\Phi_i^{(3)}(x))^2 dx \right].
\end{aligned} \tag{13}$$

In the above, ω_i and ζ_i is the natural frequency and damping ratio of the i th mode, respectively. I_i is the generalized mass, $Q_i(t)$ is the generalized force including controllable damping force $f_{er-j}(t)$, and $Q_{exi}(t)$ is the generalized force including exciting force $f_{ex}(t)$. On the other hand, the force transmitted from the input point (exciting position) to the mount position (base plate) is obtained by

$$\begin{aligned}
F_{T1}(t) &= ky(l_1, t), \\
F_{T2}(t) &= ky(l_2, t) + f_{vis-2}(t) + f_{er-2}(t), \\
F_{T4}(t) &= ky(l_4, t) + f_{vis-4}(t) + f_{er-4}(t), \\
F_{T5}(t) &= ky(l_5, t).
\end{aligned} \tag{14}$$

4. Controller design

Among many potential controller candidates, an optimal controller which is very effective for structural vibration control is adopted [19]. Considering the boundary conditions of the proposed structural system, the first and second modes are chosen to be dominant for vibration characteristics. Thus, the control model is written in the state space as follows:

$$\begin{aligned} \dot{x}(t) &= Ax(t) + Bu(t) + \Gamma d(t), \\ y(t) &= Cx(t), \end{aligned} \tag{15}$$

where

$$\begin{aligned} x(t) &= [q_1(t) \quad \dot{q}_1(t) \quad q_2(t) \quad \dot{q}_2(t)]^T, \\ u(t) &= [f_{er-2}(t) \quad f_{er-4}(t)]^T, \\ d(t) &= [f_{ex}(t)]^T, \\ y(t) &= [y_1(t) \quad y_2(t) \quad y_3(t) \quad y_4(t) \quad y_5(t)]^T, \end{aligned}$$

$$A = \begin{bmatrix} 0 & 1 & 0 & 0 \\ -\omega_1^2 & -2\zeta_1\omega_1 & 0 & 0 \\ 0 & 0 & 0 & 1 \\ 0 & 0 & -\omega_2^2 & -2\zeta_2\omega_2 \end{bmatrix}, \quad B = \begin{bmatrix} 0 & 0 \\ \frac{\Phi_1^{(2)}(l_2)}{I_1} & \frac{\Phi_1^{(2)}(l_4)}{I_1} \\ 0 & 0 \\ \frac{\Phi_2^{(2)}(l_2)}{I_2} & \frac{\Phi_2^{(2)}(l_4)}{I_2} \end{bmatrix}, \tag{16}$$

$$\Gamma = \begin{bmatrix} 0 \\ \frac{\Phi_1^{(2)}(l_{ex})}{I_1} \\ 0 \\ \frac{\Phi_2^{(2)}(l_{ex})}{I_2} \end{bmatrix}, \quad C = \begin{bmatrix} \Phi_1^{(1)}(l_1) & 0 & \Phi_2^{(1)}(l_1) & 0 \\ \Phi_1^{(2)}(l_2) & 0 & \Phi_2^{(2)}(l_2) & 0 \\ \Phi_1^{(2)}(l_3) & 0 & \Phi_2^{(2)}(l_3) & 0 \\ \Phi_1^{(2)}(l_4) & 0 & \Phi_2^{(2)}(l_4) & 0 \\ \Phi_1^{(3)}(l_5) & 0 & \Phi_2^{(3)}(l_5) & 0 \end{bmatrix}.$$

Table 1 shows the modal frequencies, damping coefficients, generalized masses, and mode shape values used in the system matrices in Eq. (16).

The control purpose is to regulate unwanted vibrations of the beam structure with appropriate control input voltage. Thus, the performance index to be minimized is chosen by

$$J = \int_0^\infty \{x(t)^T Qx(t) + u(t)^T Ru(t)\} dt, \tag{17}$$

where Q is the state weighting semi-positive matrix, and R is the input weighting positive matrix. Since the system (A, B) in Eq. (15) is controllable, we can obtain the following state feedback controller:

$$u(t) = -R^{-1}B^T Px(t) = Kx(t). \tag{18}$$

Table 1
Parameters of state space model for beam structure

	1st mode		2nd mode	
Modal frequency (rad/s)	ω_1	197.8	ω_2	526.3
Modal damping	ζ_1	0.004	ζ_2	0.0045
Generalized mass	I_1	11.3	I_2	12.4
Mode shape at l_1	$\Phi_1^{(1)}(l_1)$	1.68	$\Phi_2^{(1)}(l_1)$	1.44
Mode shape at l_2	$\Phi_1^{(2)}(l_2)$	-0.59	$\Phi_2^{(2)}(l_2)$	-1.51
Mode shape at l_3	$\Phi_1^{(2)}(l_3)$	-1.26	$\Phi_2^{(2)}(l_3)$	0
Mode shape at l_4	$\Phi_1^{(2)}(l_4)$	-0.59	$\Phi_2^{(2)}(l_4)$	1.51
Mode shape at l_5	$\Phi_1^{(3)}(l_5)$	1.68	$\Phi_2^{(3)}(l_5)$	-1.44

In the above, K is the state feedback gain matrix, and P is the solution of the following algebraic Riccati equation:

$$A^T P + PA - PBR^{-1}B^T P + Q = 0. \tag{19}$$

Since the state $q_i(t)$ and $\dot{q}_i(t)$ are not available from direct measurement, we construct Luenberger observer to estimate these states. From the observability of the system (A, C) in Eq. (15), we establish the following full-order state observer:

$$\dot{\hat{x}}(t) = A\hat{x}(t) + Bu(t) + L(y'(t) - C'\hat{x}(t)), \tag{20}$$

where

$$\begin{aligned} \hat{x}(t) &= [\hat{q}_1(t) \quad \dot{\hat{q}}_1(t) \quad \hat{q}_2(t) \quad \dot{\hat{q}}_2(t)]^T, \\ y'(t) &= [y_2(t)]^T, \\ C' &= [\Phi_1^{(2)}(l_2) \quad 0 \quad \Phi_2^{(2)}(l_4) \quad 0]. \end{aligned} \tag{21}$$

In the above, $\hat{x}(t)$ is the estimated state for $x(t)$. Using the estimated states, the control damping force of the j th ER mount is obtained by

$$u_j(t) = k_{j1}\hat{q}_1(t) + k_{j2}\dot{\hat{q}}_1(t) + k_{j3}\hat{q}_2(t) + k_{j4}\dot{\hat{q}}_2(t), \quad j = 2, 4, \tag{22}$$

where k_{jk} is the state feedback gain given in Eq. (18). The proposed ER mount is semi-active. Therefore, control signal needs to be applied to the ER mount according to the following actuating condition [20]:

$$u_j(t) = \begin{cases} u_j(t) & \text{for } u_j(t)\dot{\hat{y}}(l_j, t) > 0 \\ 0 & \text{for } u_j(t)\dot{\hat{y}}(l_j, t) \leq 0 \end{cases}, \quad j = 2, 4. \tag{23}$$

Consequently, control voltage to be applied to the ER mount is given by

$$V_j(t) = E_j(t)(h_o + \hat{y}(l_j, t)) = \left[\frac{3}{4} \frac{h_o + \hat{y}(l_j, t)}{\pi R^3 \alpha} u_j(t) \right]^{1/\beta} (h_o + \hat{y}(l_j, t)), \quad j = 2, 4. \tag{24}$$

5. Results and discussion

In order to implement the optimal controller, an experimental apparatus is established as shown in Fig. 7. The flexible steel beam (length \times width \times height = 1500 mm \times 60 mm \times 15 mm) is to be externally excited by the electromagnetic exciter, and displacement sensor (non-contact proximitor) and accelerometer are used to catch the vibration signals. The signals are fed back to the microprocessor through analog/digital (A/D) converter, and depending on the signal information control voltage is determined by means of the optimal controller. The control voltage is then applied to the ER mount through high voltage amplifiers, which have a gain of 1000. In the controller implementation, the maximum voltage is limited by 4 kV for safety. The sampling frequency to realize the controller is chosen by 1.5 kHz, and the software is written by Borland C⁺⁺. On the other hand, for the measurement of the force transmissibility, two force transducers are used: one for the input force and the other for the output force at mount position (spring or ER mount position). The marks denoted by ①, ② and ③ and on the beam represents the measured points. In the controller realization, the following feedback gains are used: $k_{21} = -729$, $k_{22} = -103$, $k_{23} = -178$, $k_{24} = -38$, $k_{41} = -729$, $k_{42} = -103$, $k_{43} = 178$, $k_{44} = 38$.

Fig. 8 presents time responses of the vibration signals when the beam structure is excited by the first mode natural frequency of 31.5 Hz (= 197.8 rad/s). It is clearly seen that both displacement at the position 2 and acceleration at the position 1 are substantially reduced by activating the proposed optimal controller. It is remarked that uncontrolled response is obtained in the absence

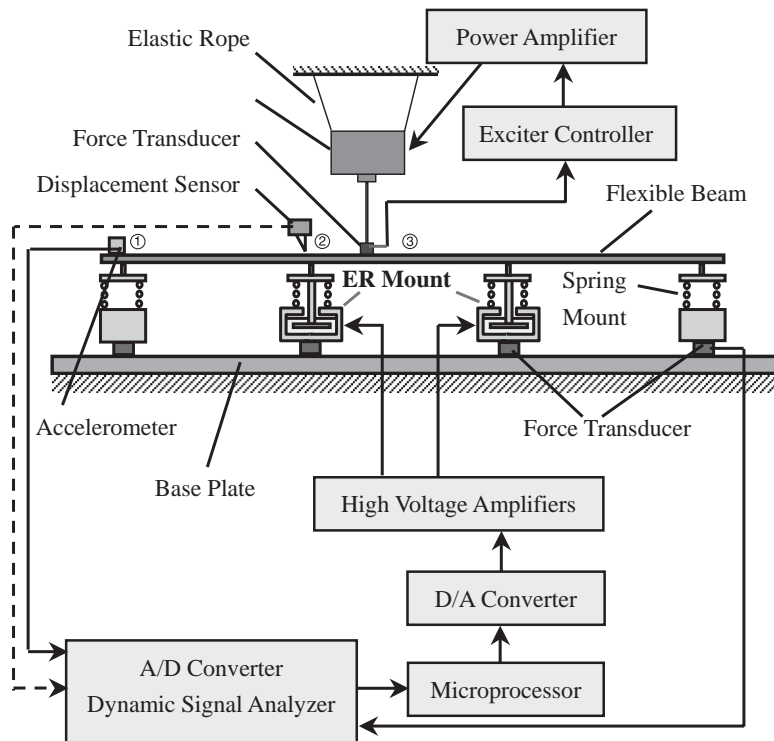


Fig. 7. Experimental apparatus for vibration control.

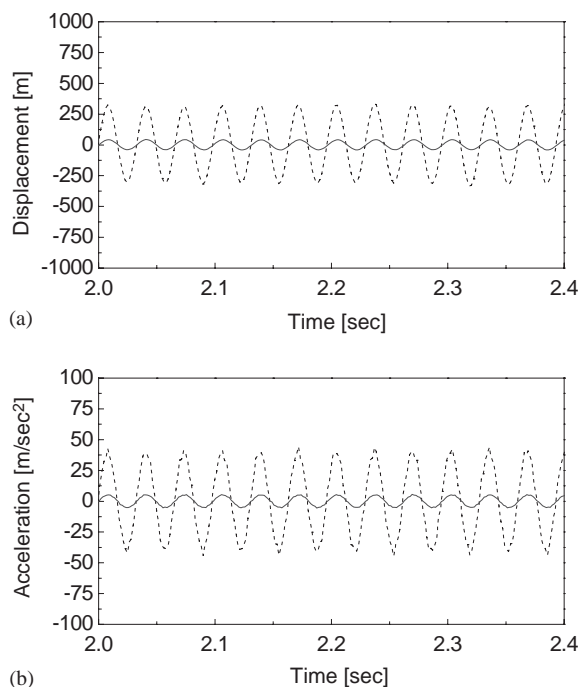


Fig. 8. Vibration responses of the beam structure in time domain: (a) displacement at position 2; (b) acceleration at position 1. - - - -: uncontrolled, —: controlled.

of the control voltage. Acceleration levels at positions 1, 2 and 3 are measured and presented in Fig. 9. We clearly observe that accelerations at the resonance frequencies are remarkably attenuated by employing the control voltage to the ER mount. Since the position 3 is the middle point of the beam structure, we do not have the second mode response.

Fig. 10 presents the force transmissibility at the spring mount and ER mount position, respectively. We figure out that the transmitted force is reduced at the spring mount position by activating the controller. However, no significant attenuation is occurred at the ER mount position. In order to explore the reason, we investigated the transmitted force at the ER mount position with constant voltages and presented in Fig. 11. It is observed that the transmitted force is increased as the voltage increases. This is mainly due to the increment of the yield stress of the ER fluid which causes the increment of the stiffness effect of the ER mount. Therefore, for the investigation of structure isolation effect, we have to evaluate the total transmitted forces by summing the transmitted forces measured at every mount position. Fig. 12 compares the total force transmissibility in the frequency domain. We see that the total transmitted force can be reduced at the resonance frequency by activating the controller. We also observe that at the off-resonance region the force transmissibility of the controlled case is almost same as the case for 0 kV. However, the isolation of the transmitted force with constant voltage is worse than the case 0 kV, especially at the off-resonance region. It is noted that the variation of the stiffness of the beam structure with or without ER effect is very small. In other words, the stiffness of the beam structure itself is larger than the increased dynamic stiffness of the proposed ER mount due to the electric field.

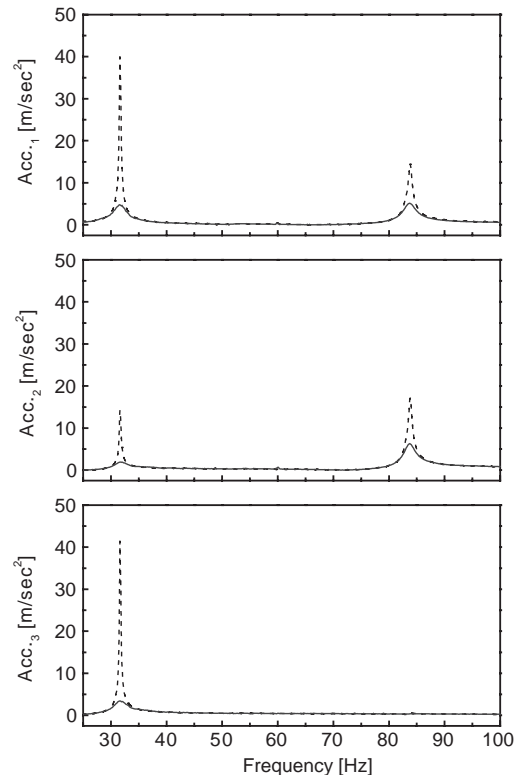


Fig. 9. Acceleration of the beam structure in the frequency domain. -----: uncontrolled, —: controlled.

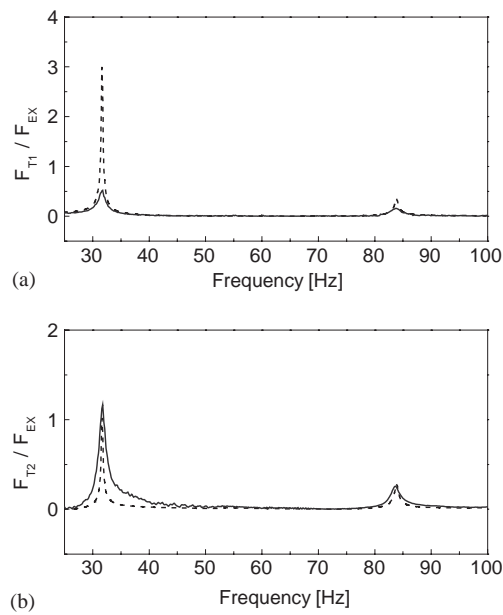


Fig. 10. Force transmissibility in the frequency domain: (a) spring mount position; (b) ER mount position. -----: uncontrolled, —: controlled.

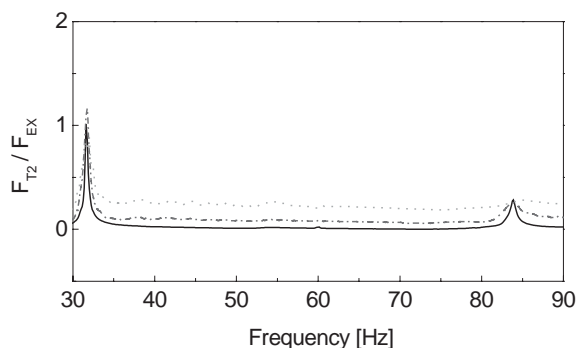


Fig. 11. Force transmissibility at the ER mount position with constant voltage. —: 0 kV, - - - -: 0.5 kV,: 1 kV.

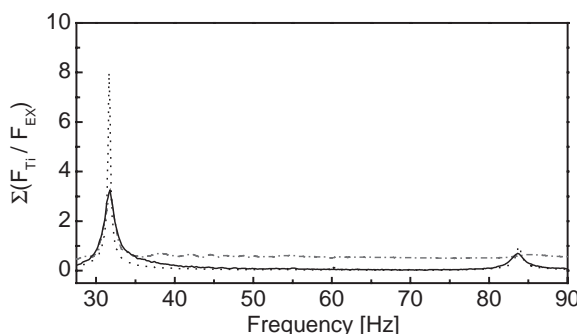


Fig. 12. Comparison of the total force transmissibility. . . .: 0 kV, - - - -: 1 kV. —: controlled.

6. Conclusion

Vibration control of a flexible beam structure supported by adaptable ER mounts was undertaken in a closed-loop control fashion. After manufacturing the squeeze mode ER mount, the field-dependent damping forces are experimentally evaluated. The ER mounts were then integrated with the beam structure to attenuate vibrations. An optimal controller associated with state estimator was designed and empirically realized. It has been demonstrated that both displacement and acceleration of the beam structure can be substantially reduced at the resonant frequencies by activating the controller. In addition, it was shown that total transmitted force can also be attenuated by employing an appropriate control voltage. The control results presented in this work are quite self-explanatory justifying that the squeeze mode ER mount can be usefully employed for vibration control of flexible structures subjected to small amplitude and high-frequency external excitations.

References

- [1] J.P. Coulter, T.G. Duclos, Application of electrorheological materials in vibration control, *Proceedings of the 2nd international Conference on ER Fluids*, Raleigh, NC, 1989, pp. 300–325.

- [2] Y. Choi, A.F. Sprecher, H. Conrad, Response of electro-rheological fluid-filled laminate composites to forced-vibration, *Journal of Intelligent Material Systems and Structures* 3 (1992) 17–29.
- [3] S.B. Choi, Y.K. Choi, C.C. Cheong, Active vibration control of intelligent composite laminated structures incorporating an electro-rheological fluid, *Journal of Intelligent Material Systems and Structures* 7 (1996) 411–419.
- [4] N.K. Petek, D.J. Romstadt, M.B. Lizell, T.R. Weyenberg, Demonstration of an automotive semi-active suspension using electro-rheological fluid, SAE Paper, 950586, 1995.
- [5] E.W. Williams, S.G. Rigby, J.L. Sproston, R. Stanway, Electrorheological fluid applied to an automotive engine mount, *Journal of Non-Newtonian Fluid Mechanics* 47 (1993) 221–238.
- [6] S. Morishita, J. Mitsui, An electronically controlled engine mount using electro-rheological fluid, SAE paper, 922290, 1992.
- [7] S.B. Choi, Y.T. Choi, Sliding mode control of shear-mode type ER engine mount, *KSME International Journal* 13 (1999) 26–33.
- [8] S.A. Austin, The vibration damping effect of an electrorheological fluid, *Journal of Vibration and Acoustics* 115 (1993) 136–140.
- [9] K.W. Wang, Y.S. Kim, D.B. Shea, Structural vibration control via electrorheological-fluid-based actuators with adaptive viscous and frictional damping, *Journal of Sound and Vibration* 177 (1994) 227–237.
- [10] S.B. Choi, Vibration control of a flexible structure using ER dampers, *American Society of Mechanical Engineers, Journal of Dynamic Systems, Measurement and Control* 121 (1996) 134–138.
- [11] G.J. Hiemenz, N.M. Wereley, Seismic response of civil structures utilizing semi-active MR and ER bracing systems, *Journal of Intelligent Material Systems and Structures* 10 (1999) 646–651.
- [12] R. Stanway, J.L. Sproston, A.K. EI-Wahed, Application of electro-rheological fluids in vibration control: a survey, *Smart Materials and Structures* 5 (1996) 464–482.
- [13] R. Stanway, J.L. Sproston, S.G. Rigby, E.W. Williams, Modeling and control of electro-rheological fluids in the squeeze-flow mode, *Proceedings of the Second International Conference on Intelligent Materials*, Williamsburg, VA, 1994, pp. 1176–1184.
- [14] R. Stanway, J.L. Sproston, A. Washed, Adaptive vibration control using the electro-rheological squeeze-flow damper, *Proceedings of SPIE* 2715 (1999) 110–120.
- [15] J. Tichy, Behavior of a squeeze film damper with an ER fluid, *STLE Journal of Tribology* 36 (1993) 127–133.
- [16] S. Morishita, J. Mitsui, Squeeze film damper as an application of ER fluid, *Proceedings of the 8th International Conference on Rotordynamics*, Lyon, France, 1990, pp. 277–282.
- [17] M.R. Jolly, J.D. Carlson, Controllable squeeze film damping using magnetorheological fluid, *ACTUATOR* 96, *5th International Conference on New Actuator*, Bremen, Germany, 1996, pp. 333–336.
- [18] S.B. Choi, High damping mechanism for structural systems using ER mounts, Technical Report for Korea Agency for Defense Development, 2001, 7–16.
- [19] S.B. Choi, W.K. Kim, Vibration control of a semi-active suspension featuring electrorheological fluid dampers, *Journal of Sound and Vibration* 234 (2000) 537–546.
- [20] G. Leitmann, Semiactive control for vibration attenuation, *Journal of Intelligent Material Systems and Structures* 5 (1994) 841–846.